16th ICAAR LISBOA 2020-2022

16th International Conference on
Alkali-Aggregate Reaction in Concrete
Lisboa | LNEC | Portugal | 31 May - 2 June 2022

http://icaar2020-2022.lnec.pt

Stiffness damage testing of laboratory-cast alkali-silica reactive concrete and cores drilled from an existing concrete structure

Kathrine Mürer Stemland [(1)], Eva Rodum [(2)], Terje Kanstad [(3)]

(1) NTNU, Trondheim, Norway, kathrine.stemland@ntnu.no

(2) Norwegian Public Roads Administration, Trondheim, Norway, eva.rodum@vegvesen.no

(3) NTNU, Trondheim, Norway, terje.kanstad@ntnu.no

Abstract

The results presented in this paper are part of an experimental programme in a project on the structural effects of alkali-silica reactions (ASR) in concrete. Our main objective was to establish the relationship between the expansion of concrete due to ASR and its related degradation when tested under accelerated ASR conditions in the laboratory and verify whether the same relationship also applies for concrete from existing ASR-affected structures. Our aim was to determine the expansion of existing structures, which is necessary for the calculation of the structural effects due to ASR.

We tested several cylinders and cubes, both free and restrained, cast with alkali-silica reactive concrete, and exposed to accelerated conditions (38 °C and 100% RH). We drilled core samples from various parts of the Elgeseter Bridge in Norway, a historically protected 200 m long beam bridge from 1951 which is heavily attacked by ASR.

We used a particular mechanical test method, the "Stiffness damage test" (SDT), which consists of cyclic compressive loading of cylinders, to characterize the material degradation of the laboratory samples and the drilled cores from Elgeseter Bridge. The relationship between the SDT output parameters and the expansion measured in the laboratory samples was then used to determine the expansion of the Elgeseter specimens. The results show a good correlation with previous expected expansions and measurements on the bridge, and we refined the results using the stiffness damage index (SDI), which improved the reliability of SDT as a useful tool for determining the structural effects of ASR in an existing structure.

Keywords: Alkali-silica reaction (ASR); Concrete degradation; Concrete expansion; Stiffness damage test (SDT); Stiffness damage index (SDI)

1. INTRODUCTION

One of the essential tasks of structural engineers today is to maintain the structural safety and serviceability of existing structures. This is due to both economic and environmental reasons as a very large number of structures reach the end of their assumed service life. An existing structure was designed so that the structural resistance satisfactorily exceeds loads in terms of the structural safety requirements at the time. However, structural resistance may decrease due to loss of mechanical properties, and the load effects may increase. Alkali-silica reaction (ASR) can contribute to both, leading to a shorter service life.

ASR is a deterioration mechanism in concrete caused by chemical reactions between alkali-reactive aggregates (SiO_2) and alkalis in the pore water in the cement paste (Na+, K+). The reaction product is an alkali-silica gel that swells when exposed to water. This mechanism leads to an expansion of the concrete, resulting in micro-cracking and the deterioration of various mechanical properties. Since the reinforcement is bonded to the concrete in a reinforced concrete structure, the expansion of the concrete itself will create internal stresses in a section. Similar stress states will also occur if one part of a section expands more than other parts. If the structure is statically indeterminate, e.g., restrained against the ASR expansion, these stresses will also result in additional load effects in the form of restraining moments and axial forces.

To calculate the strain and load effects in a section, we need to know the magnitude and distribution of the ASR expansion. This is difficult to determine in an arbitrary structure without any expansion measures. One of the main objectives of this project therefore was to establish a relationship between

the expansion and the related concrete deterioration of laboratory specimens that can then be applied to the existing structure. Previous work [1-9] has shown promising results for various damage parameters, using both destructive and non-destructive tests such as tensile/compressive strength tests, petrographic analysis such as the damage rating index (DRI), and the stiffness damage test (SDT). This last test was used to assess the damage of the concrete and is further discussed in this paper.

The assessment of Elgeseter Bridge is included as part of this project. The level and distribution of the expansion in the structure and the degradation of the mechanical properties of the concrete are important input parameters for the structural analysis. Several cores were drilled from different parts of the bridge and SDT tested. The results from these tests are presented and compared with the results from the SDT of the accelerated laboratory specimens.

2. STIFFNESS DAMAGE TEST

The stiffness damage test (SDT) is a mechanical stress-strain test consisting of five load cycles on a specimen up to a specific load level, as illustrated in Figure 2.1. The test was initially developed as a non-destructive test at low load levels (5.5 MPa) so that the samples could be successively re-tested either at other expansion levels or for other parameters [1, 2]. The original idea of the test was that, for a damaged sample, the initial loading modulus would be significantly lower than the first part of the unloading modulus, which could represent the stiffness of the uncracked concrete. The difference between the loading and unloading modules creates an energy dissipation (hysteresis) which can be directly related to microcrack activity [1]. For an undamaged sample, the loading and unloading modulus would be quite similar. Several studies have subsequently evaluated and tried to quantify both the test procedure and the output parameters that give the best measure of damage [1-3, 5, 8, 9]. One of the main reported problems with the test is that the relationship between the damage parameters and the expansion varies for different types of aggregates and concrete mixes (concrete strengths).

Sanchez et al. [5] tested different input parameters, such as loading levels, aggregate types, and concrete mixes, to verify their influence on the test results. In this study, a loading level of 40% of the 28-day compressive strength was found to give more reliable results than fixed loading levels, and this load level caused no additional damage to the samples. Various output parameters were also evaluated, and best results came from the hysteresis area (HA), which was assumed to be the energy used to close the macro and microcracks under the load cycles, and the plastic deformation (PD), which is the permanent strain applied to the samples by the loading of all five loading/unloading cycles. The secant E-modulus of the second and third load cycles was also found to be a promising parameter and was especially sensitive to small expansions.

The same authors [6] went on to investigate the use of indices, such as the stiffness damage index (SDI) and the plastic deformation index (PDI), instead of the absolute output parameter values (HA, PD and E-modulus). The way they calculated the SDI value is shown in Equation (1). This value is the ratio between the sum of the hysteresis or dissipated energy (SI) and the total applied energy to the system (SI+SII) for the five cycles. The areas representing these values are illustrated in Figure 2.1. This ratio expresses the amount of the applied energy that the system consumes. The authors argued that the absolute value parameters (HA, PD and E-modulus) would depend on the amount of energy applied to the system, which could be increased with increasing design strengths. This makes them more dependent on the actual 28-day concrete strength, which is not necessarily known for an existing structure, than the indices (SDI/PDI) when deciding the loading level of the test. They concluded that the indices would provide a better understanding of damage generation as the ASR expansion develops and better represent damage for different materials.

The test method and damage parameters investigated by Sanchez et al. [5-7] were used by Kongshaug et al. [8] in experimental work carried out at NTNU. The experimental work presented in this paper is a continuation of the same work, so the same method was chosen for our study as well. Section 5 describes the test procedures more thoroughly. The output parameters presented in this paper are the SDI values and the average secant E-modulus of the last loading and unloading cycle (cycle number 5). After five cycles, the values of the loading and unloading secant E-moduli approach each other. This value, therefore, is probably the best estimate for the stiffness of the damaged concrete. The average E-modulus of the second and third cycle was selected by Sanchez et al. [5] based upon the test procedure for the E-moduli of ordinary concrete. This is, however, not necessarily applicable to damaged concrete.

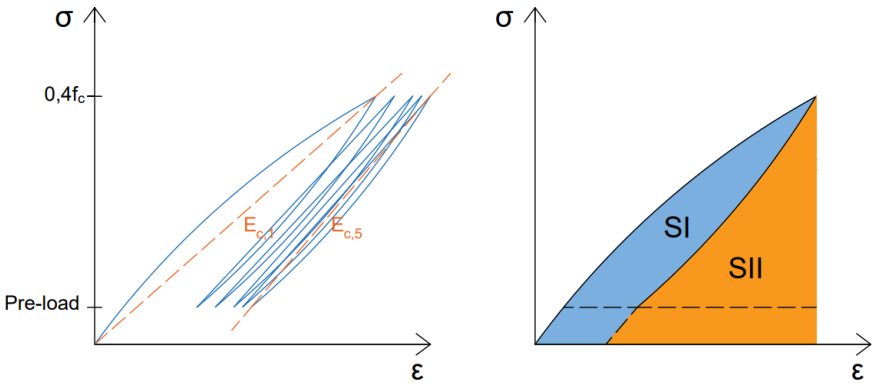

Figure 2.1: left: Illustrated stress-strain curve from the SDT, right: Areas representing the dissipated energy (SI) and the total applied energy (SII)

$$SDI = \frac{\sum_{i=1}^{5} SI_i}{\sum_{i=1}^{5} (SI_i + SII_i)} \quad (1)$$

SDT is not yet a fully developed and reliable method for the assessment of the expansion and degradation of an ASR-exposed concrete. Even with an adjusted test procedure, the results in [7] still show significant variation between the SDI/Expansion relationships for different types of aggregates and concrete mixes. The main goal of this investigation therefore is not to find the final values for the ASR expansions and the deterioration of the concrete in Elgeseter Bridge, but merely to indicate what these values might be if the SDI results of the cores are related directly to the accelerated laboratory specimens.

3. ELGESETER BRIDGE

Located in Trondheim in Norway, Elgeseter Bridge is a concrete beam bridge opened in 1951. The bridge was protected as part of the Norwegian cultural heritage in 2008. The bridge is 200 m long and consists of nine spans with four T-beams supported by four columns in each of the axes 2-9, as shown in Figure 3.1. The superstructure is fixed at the abutment towards the south and free with a dilation joint at the northern abutment.

Elgeseter Bridge is the most investigated bridge in Norway regarding ASR, which was first diagnosed in 1990. Since then, the bridge has been subjected to frequent surveys and various mitigating and repair actions [10]. The expansion of the concrete has led to vertical cracking of the columns, closure of the joint in axis 10, displacement (tilting) of the columns, and delamination of the bridge deck. Renovation work in 2014-15 and recalculations of its load-bearing capacity meant the bridge was included in several R&D activities carried out by the NPRA, partly in collaboration with NTNU, SINTEF and Université Laval in Canada. The results from examinations of moisture content and cracking on Elgeseter Bridge up to 2015 were summarized by Rodum et al. [11]. Its elongation at the northern abutment has been estimated based on global movements (closure of the joint and displacement of the columns in axis nine) to be about 200 mm. In strain, this corresponds to about 1000 με or 1 mm/m (‰). The main uncertainty in this case therefore is connected to the distribution of the expansion over the cross section.

A visual inspection in 2012 revealed signs (white surface precipitations) suggesting that the outer part of the plate (Plate 1) was moister than the inner part (Plate 2), probably due to damage in the membrane after a previous extension of the pavements leading to leakage through the concrete [12]. This was confirmed by determination of the degree of capillary saturation (DCS) in cores drilled from the top of the plate at three different locations along the bridge (A, B and C in Figure 3.1) [11]. The average DCS value in depth 0-150 mm was very high in the outer/western parts of the plate (98-99%), considerably higher than in the inner part where the DCS also increased from location A (79%) to B (90%) to C (97%). Visual examination of plane polished sections prepared from cores from the same locations showed a relationship between the moisture state and the crack extent [11]. Due to both the moisture condition in the plate and the heavier weather exposure (rain, sun) from the west, the outer beam (Beam 1) on the western side was also suspected to be moister than the inner beam (Beam 2).

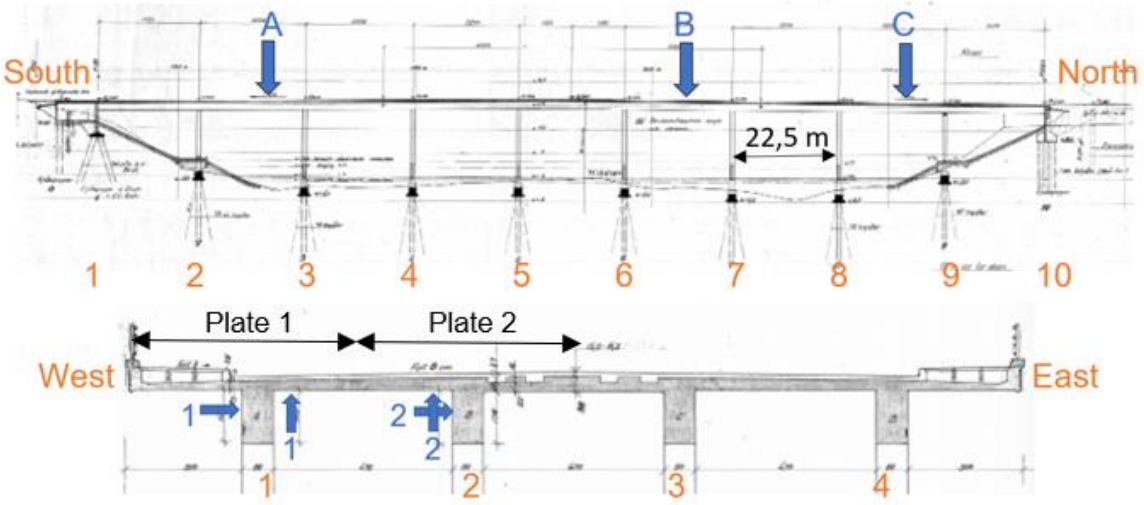

Figure 3.1: Structural system and cross section of the bridge. The locations of the cores from 2020 are marked with blue arrows.

3.1 Drilled cores from Elgeseter Bridge

Cores for SDT testing were drilled from the same locations A, B and C as the cores drilled in 2014, see Figure 3.1. In each location, three cores were drilled from each of Plate 1 and Plate 2, and two cores were drilled from each of Beam 1 and Beam 2 (and an extra core was drilled from location A/Beam 2). The cores from the plates were drilled vertically from the bottom and up, while the cores from the beams were drilled horizontally in the middle of the web where there was almost no reinforcement (and loading stresses were also small in that direction). All the cores had a diameter of ≈ 95 mm.

Table 3.1: Overwiev of the extracted cores and the associated specimens prepared for SDT

Location	Structural member		Cores		SDT specimens	
			Number	Dimensions (d/l), (mm)	Number	l/d-ratio
A	Beam	1	1	95/800	3	2, 2, 2
		2	2	95/800, 95/800	6	2, 2, 2, 2, 2, 2
	Plate	1	2	95/130*), 95/130	2	1,32, 1,32
		2	1	95/190	1	1,80
B	Beam	1	2	95/800, 95/800	4	2, 2, 2, 2
		2	1	95/800	3	2, 2, 2
	Plate	1	2	95/130*), 95/170*)	2	1,27, 1,64
		2	2	95/190, 95/210	2	1,85, 2
C	Beam	1	2	95/800, 95/800	4	2, 2, 2, 2
		2	2	95/800, 95/800	4	2, 2, 2, 2
	Plate	1	2	95/130*), 95/160*)	2	1,53, 1,27
		2	2	95/190, 95/200	2	1,85, 2

*) Significant cracking observed on cores

For the beams, one of the "twin" cores was tested for SDT (two from location A/Beam 2) and the other for DRI. The cores were drilled through the 800 mm width of the web. Approximately 100 mm of the outer part of each core end was cut off. This made it possible to make three test specimens with an l/d ratio of 2 from each core. The specimens were marked "west," "middle," and "east" to keep track of

which part of the core each specimen originated from. Three specimens from three of the DRI-cores were also SDT tested. All the cores from the plate were also SDT tested. The drilling was more challenging in the plate due to the position of both transversal and longitudinal reinforcement and a higher level of deterioration. The thickness of the plate is only about 280 mm. It was therefore only possible to make one test specimen from each core. The cores had various lengths, and the l/d ratio of these specimens varied from 1.27 to 2 (specified for each specimen in Table 3.1). The measuring length in the SDT tests was adjusted proportionate to the l/d ratios, from 100 mm for the l/d=2.

All the cores were wrapped in plastic immediately after drilling and kept moist at 5 °C prior to sawing and testing. Each core was thoroughly examined before preparation of specimens, i.e., recording cracks, reinforcement, reaction rims, and visible ASR gel. There were a total of 24 test specimens for SDT from the beams and 11 from the plates. An overview of the specimens is shown in Table 3.1.

4. LABORATORY SPECIMENS

The laboratory samples presented here consist of fourteen 230 mm cubes and ten 150x300 mm cylinders. In addition, twenty-four 100 mm cubes were cast for testing of compressive strength. An overview of the samples is shown in table 4.1. These samples are a part of the first of two comprehensive laboratory programmes considering the structural effects of ASR. One of the main aims of these programmes was to investigate the effect of external compression and internal reinforcement on ASR expansion and the corresponding deterioration of the mechanical properties. These effects are not further discussed in this paper but will be included in impending work.

The concrete mix used for these samples is intended to be representative for Norwegian bridges built in the 1950-60s and has previously shown an adequate expansion rate in accelerated ASR tests [13]. The mix contains alkali-reactive coarse aggregate from crushed cataclasite (Ottersbo 4/16 mm), non-reactive sand mainly consisting of granite and gneiss (Årdal 0/4 mm), 457 kg/m^3 ordinary Portland cement (Norcem Industri, CEM I 42.5R with 1.24% Na_2O_{eg}), and a w/c ratio of 0.48. This gives an alkali content of 5.6 kg Na_2O_{eq}/m^3. After casting, all the samples were kept wrapped in wet burlaps under plastic at 20 °C for 28 days. From 28 days of age, the samples assumed to expand were stored in tight plastic buckets with 100% RH (on grids above water with the bucket walls covered with wet burlaps) at 38 °C. Reference samples were stored in a similar way at 20 °C (causing negligible ASR). Most of the expanding and all the reference samples were free in all directions. Five of the 230 mm cubes, however, were loaded in the z-direction by a compressive stress of 3 MPa during the exposure. The load-cells used are the same as described by Kongshaug et al. [8].

The expansion of the 230 mm cubes was measured between studs glued to the concrete surfaces at intervals of 200 mm by means of a Digital DEMEC Mechanical Strain Gauge instrument with measuring accuracy down to 0.001 mm. This gives a theoretical strain measurement accuracy of 0.005 E-3. The expansion was measured on all surfaces (in x, y, and z-directions). The expansion of two of the 230 mm cubes, one free and one restrained, was measured regularly throughout the whole test period to keep control of the expansion rate and form a basis for the intended expansion levels of the other cubes. The expansion of the other 230 mm cubes was only measured prior to the exposure in the 38 °C room (zero readings) and just after the cubes were taken out for testing (after cooling). The expansion of the cores drilled from the cubes was assumed to be the same as the expansion of surfaces parallel to the drilling direction.

SDT tests were performed on 100x200 mm cores drilled from the free and loaded 230 mm cubes at pre-decided expansion levels. Two cores were drilled from the free cubes and four from the restrained cubes (two cores in both the restrained and one of the free directions). The expansion levels that were tested were 0.5, 1.5, 2.0 and 3.0‰ (approximate levels; exact levels were determined for each cube prior to the drilling of cores). Cores from the “undamaged” reference cubes at 20 °C were also tested at the same time as the ASR-affected ones.

The expansion of the 150x300 mm cylinders was also measured regularly and at the time of testing. Bow-shaped Mitutoyo extensometers were used for this in the longitudinal and radial directions, respectively. These cylinders were SDT tested directly, two parallel cylinders at each of the approximate expansion levels 1.5 and 2‰. Four cylinders were also stored at 20 °C and tested as references.

Table 4.1: Overview of cubes (FP38, RP38, FP20), cast cylinders (S38, S20) and cylinders drilled from cubes

Mark	Number	Size	Load (z-dir.)	Temperature [°C]	RF	Number and dir. of drilled 100x200 mm SDT specimens from the cubes
FP38	5	$(230\ mm)^3$	-	38	~100%	2 (z-dir.)
RP38	5	$(230\ mm)^3$	3 Mpa	38	~100%	2 (z-dir.), 2 (y-dir.)
FP20	4	$(230\ mm)^3$	-	20	~100%	2 (z-dir.)
S38	6	300x150 mm	-	38	~100%	-
S20	4	300x150 mm	-	20	~100%	-

5. TEST PROCEDURES

5.1 Stiffness Damage Test (SDT)

As described in section 2, the test consists of five load cycles up to a level that is approximately 40 percent of the static strength of the concrete. Sanchez et al. [5-7] refer to this strength as the 28-day compressive strength, but that strength is often unknown in existing structures. That is why it is desirable to make some initial static tests on the structure to determine its load level. Sanchez et al. [6] also discussed this and suggested that if the 28-day strength was not known the load level should be based on compressive strength tests from an undamaged part of the structure. During the repair work on Elgeseter Bridge in 2015, cores were drilled from the concrete plate to determine the compressive strength. The mean value of six specimens (cylinders with l/d ratio 2) was 37 MPa, and this value was initially chosen as the basic value, for both the plate and beams. Nevertheless, the spread in the compressive strength from different cores meant that the load level in some cases exceeded 40% of this strength. Since there were several specimens from the same location, the operator had the option of adjusting the load level for some specimens. This will be further assessed in the discussion. For the lab samples, we used a constant load level based on the measured 28-day strength. Apart from this, the test procedure was the same for all the specimens, both the lab samples and the cores extracted from the bridge.

In the test, the cylinder is equipped with a strain-rigg that measures the longitudinal displacement along three generatrices with an angle of 120° between them. For cylinders with l/d=190/95, the displacement is measured over a length of 100 mm symmetrically about the middle plane of the cylinder. For the shorter cores from the bridge deck the measuring length was shortened to 65 (l/d =1.27-1.32) and 80 (l/d=1.53-1.64), respectively. For the cast cylinders (l/d=300/150) the measuring length was 150 mm. The stress-strain relationship is recorded during the test to obtain stress-strain curves. The specimen is pre-loaded to an initial load of 10 kN, which for cylinders with d≈95 mm corresponds to a stress of 1.4 MPa, and then loaded cyclically five times between this level and 40% of the basic compressive strength (28-day laboratory samples or field samples). The loading rate in the cyclic tests is 0.1 MPa per second. A Form Test Alpha 3 hydraulic press was used for all the 95 mm cylinders, and a Losenhausen BP500 was used for the 150x300 cylinders. The SDI value (Equation (1)) and the secant E-moduli can be calculated from the stress-strain curves.

5.2 Work diagram and compressive strength test

After completing SDT, the cylinders (from both the lab series and bridge cores) were tested deformation controlled to failure to determine their stress-strain relationship and compressive strength. The cylinders were run with a loading rate of 0.3‰ strain per minute until failure. The test procedure is described in NS 3473, Appendix A pt. A.11.3 and a Losenhausen BP500, 500 kN press was used for the loading.

The compressive strength of the laboratory specimens was determined from the 100 mm cubes from the same batch as the test specimens. Three cubes stored in water at 20 °C were tested at 28 days. Furthermore, six cubes, three stored at 38 °C and three at 20 °C in the same buckets as the free cubes, were tested at each expansion level. The loading rate in these tests was 0.8 MPa per second, in accordance with NS-EN 12390-3. A Toni Technik model 2031 hydraulic load frame was used. The reference cylinder strength for the SDT of the laboratory cast samples was 80% of the 28-day cube

strength. The average cylinder strength was 54 MPa, which corresponds to a maximum stress in the SDT of 22 MPa.

6. RESULTS

6.1 Laboratory specimens

The SDI of the cylinders that were drilled from the 230 mm cubes at different expansion levels are plotted against their corresponding expansions to the left in Figure 6.1. Only cylinders from unloaded directions are included. Each point is the average of two cores with relatively low spread; the average coefficient of variation (CV) is 3.6%. The blue, orange, and grey points are the results from the free cubes stored at 20 °C (FP20), 38 °C (FP38), and the loaded cubes stored at 38 °C in the directions perpendicular to the loading (RP38-Y), respectively. The light blue and green points are the results of the 150x300 mm cylinders stored at 20 °C (S20) and 38 °C (S38). This figure shows that the SDI values increase quite linearly up to about 0.25 at an expansion level of about 2.5‰. Above that expansion level the SDI values seem to level out. A curved regression line will therefore be a better fit to the results when the complete dataset is included, and a linear regression line can only be plotted to an expansion of about 2.5‰.

The reduction in the E-modulus from the fifth cycle with the expansion of the identical specimens is shown to the right in Figure 6.1. The average CV of the two specimens here is 1.6%. In this case, the reference E-modulus is based on the mean secant stiffness in the fifth cycle of the specimens that were stored at 20 °C. The expansion of these specimens is small, and the reduction of the E-modulus (due to this expansion) is therefore also small. The E-moduli of this cycle for the 95x190 mm cylinders drilled from the cubes increased from 31 500 MPa to 34 000 MPa from the age of 120 days to about 425 days. The 150x300 mm cylinders were about 34 000 MPa at both these ages. The increase was relatively uniform with the increase in age for the 95x190 mm cylinders stored at 20 °C. This development was expected to go faster for the specimen stored in the 38°C room, so the reference E-modulus was chosen as 34 000 MPa as an average value for the whole test period of the specimens in this investigation.

The E/E_{ref} gradually decreases with the expansion. As with the SDI, the progression is quite linear up to an expansion level of about 2.5-3.0‰. From that level, the further reduction in the E/Eref seems to be small. These results therefore also fit better to a curved than to a linear line, and the linear regression is only plotted to an expansion of 2.5‰.

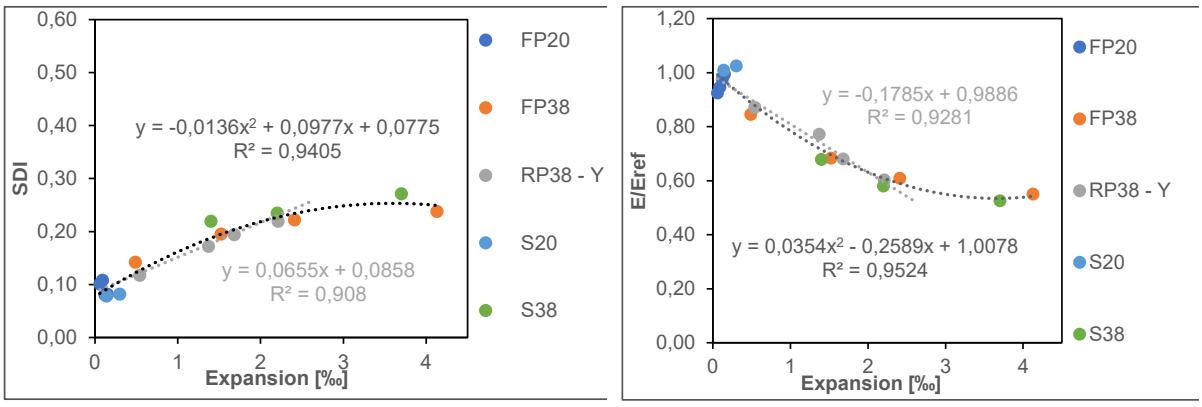

Figure 6.1: Development of the SDI values (left) and E/E_{ref} ratio (right) with the expansion of the specimens in the laboratory series. Polynomial and linear best-fit regression curves are plotted in black and grey respectively as simplified descriptions of the results. The blue, orange, and grey points represent the free cubes stored at 20 °C (FP20), 38 °C (FP38), and the loaded cubes stored at 38 °C in the directions perpendicular to the loading (RP38-Y), respectively. The light blue and green points represent the 150x300 mm cylinders stored at 20 °C (S20) and 38 °C (S38).

6.2 Elgeseter Bridge

The average results of the SDT cores from Elgeseter Bridge are shown in Table 6.1. The first columns show the location and structural member of the cores, and the successive columns show the secant E-modulus for the first and the fifth cycles together with the ratio between the latter and a selected

reference E-modulus, followed by the SDI, the compression strength from the final static tests, and the post-calculated load levels based on this strength. The number of specimens used for the average values for each part is described in Table 3.1. The CV values varied between 0.02-7.8%, 2.34-14.93% and 1.45-14.85% with average values of 4.9, 9.0 and 6.76% for the fifth secant E-modulus, the SDI value, and the compressive strength, respectively.

In this case, the reference E-modulus was based on the fifth secant E-modulus from the SDT on the cores from Beam 2, which was assumed to be the least damaged structural member. The average SDI values in the three locations of this beam were 0.13, 0.13, and 0.16, and the corresponding E-moduli were 25800, 26300, and 23500 MPa, respectively. The reference E-modulus should therefore be somewhat higher since it is probable that this beam also has a certain expansion. The SDI for the unaffected laboratory specimens was 0.08, but this value could vary with the concrete quality. The lowest and highest values for the fifth secant E-modulus of the single specimens from Beam 2 were 21000 and 28000 MPa, with corresponding SDI values of 0.17 and 0.14. Based on the laboratory specimens tested, these values correspond to an expansion in the range of 0.5 to 1‰ and a reduction of the E-modulus by 10-20%. However, the lowest E-modulus in this sample was especially low, and the mean of all the twelve specimens was about 25500 MPa. So, we set the reference E-modulus for this concrete at 28000 MPa, which is the mean of the fifth cycle of all the tested specimens from Beam 2 multiplied by a factor of 1.1.

Table 6.1: Average results for each structural member

Location	Structural member		Ec,1 [MPa]	Ec,5 [MPa]	Ec,5/Ec,ref	SDI	fc [MPa]	Load %
Area A	Beam	1	12802	16341	0.58	0.23	24.0	61.1
		2	23279	25830	0.92	0.13	38.9	41.5
	Plate	1	5518	10290	0.37	0.36	29.9	37.1
		2	12274	15145	0.54	0.22	32.1	48.7
Area B	Beam	1	22162	24599	0.88	0.14	40.7	39.4
		2	23404	26273	0.94	0.13	38.8	42.8
	Plate	1	5787	9880	0.35	0.36	28.4	46.9
		2	19992	22881	0.82	0.16	40.1	40.2
Area C	Beam	1	14339	16757	0.60	0.19	27.9	54.1
		2	20330	23530	0.84	0.16	39.2	40.7
	Plate	1	3820	7010	0.25	0.39	27.4	42.4
		2	21569	23773	0.85	0.15	47.1	33.8

Figure 6.2 shows the average results for the SDI and E/E_{ref} values plotted for each structural member in each location. The values are plotted as orange and blue columns related to the left vertical axis. The corresponding estimated expansions based on the equations in Figure 6.1 are also plotted for the same structural members with grey and black markers for the linear and polynomial regression lines, respectively. They are related to the right vertical axis. The results show a consistently higher SDI value and reduction of the E/E_{ref} ratio for the plate in the outer part of the cross-section (Plate 1) than for the plate in the inner part (Plate 2) for all locations. Plate 2's SDI and E/E_{ref} ratio are so high/low that they fall beyond the polynomial regression curve from the lab specimens. An elongation of the linear expression for both the SDI and E/Eref was therefore used to estimate the expansion. Beam 1 also shows a higher SDI value and lower E/Eref than Beam 2, especially in areas A and C. In area B, the differences between Beam 1 and Beam 2 are less significant. The results from the plates clearly correspond with the findings of Rodum et al. [11] concerning the moisture content and extent of internal cracking, and their hypothesis about the expansion level being higher in the outer Beam 1 than in the more sheltered Beam 2 is also supported.

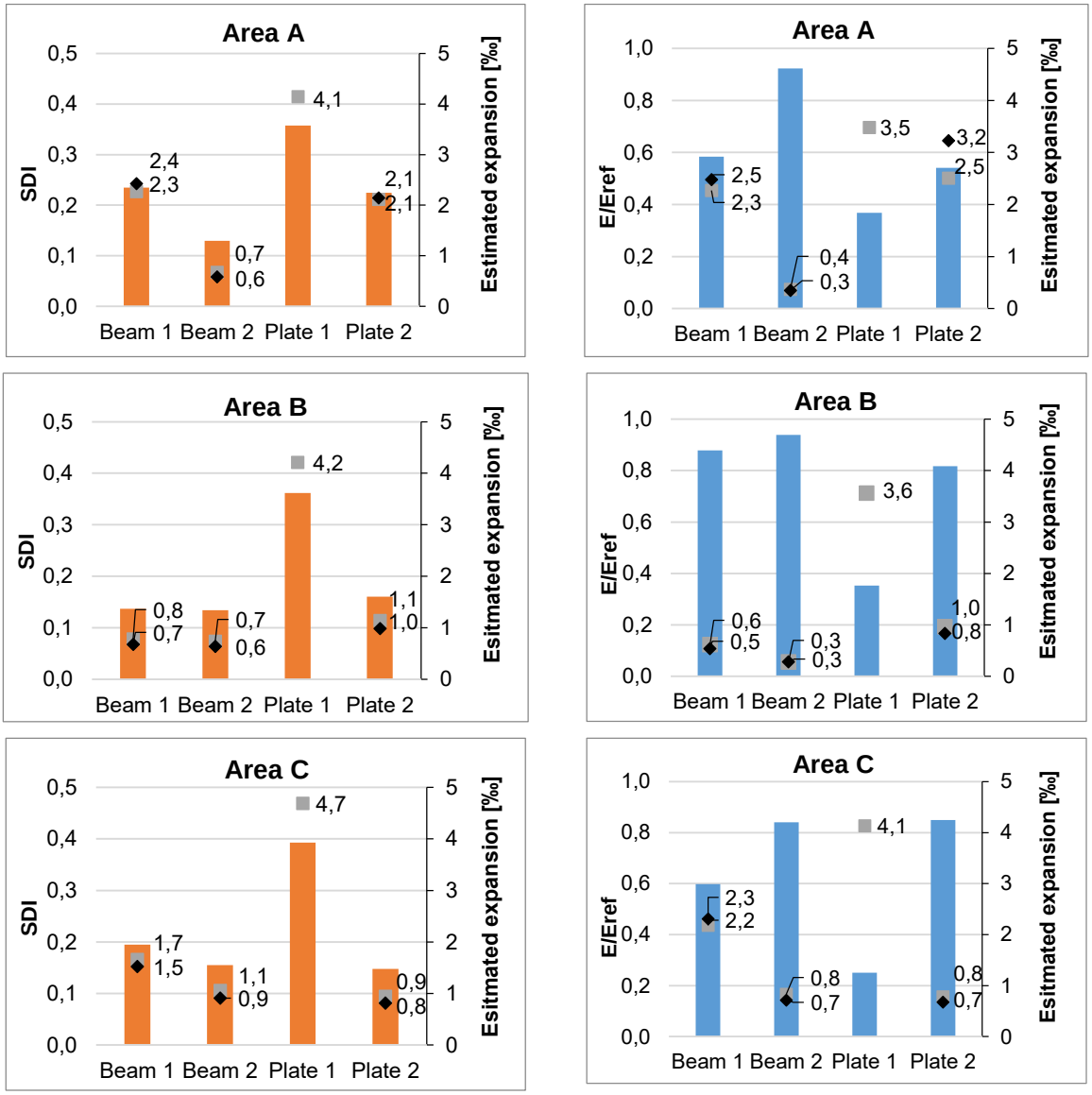

Figure 6.2: Average values for SDI (left) and E/E_{ref} (right) for the different structural parts on Elgeseter Bridge in orange and blue columns, respectively. Estimated expansion based on linear and polynomial regression lines from Figure 6.1 plotted for the same locations with grey and black markers.

7. DISCUSSION

The main results from the SDT testing of the laboratory specimens are the relationships between the expansion and the parameters SDI and E/E_{ref}, respectively. These results are plotted in Figure 6.1. The development of both parameters is quite linear up to an expansion of about 2.5‰, where they start to level off. However, the number of data points beyond this level is low, which makes it difficult to predict further development. Nevertheless, the most likely outcome is that the SDI and E/E_{ref} do not reach a specific limit but continue to increase/decrease with further expansion. Similar development of the results has previously been reported in [3, 5, 6, 8].

The SDI calculation according to Equation (1) sums the dissipated energy in all five load-cycles and divides it by the total applied energy of the same cycles, making this value an expression of a sort of average dissipated energy intensity. Even if there is no energy dissipation in the last cycles, the denominator will increase, and the index will tend towards zero if the number of cycles is increased. This is not logical if the intention is to express a degree of damage in the material. An alternative SDI expression was therefore proposed in a master's thesis by Oseland [14] based on Kongshaug et al. [8], in which the ratio between the dissipated and applied energy in each cycle is summed. This expression

will tend towards a value that increases with the number of cycles, but where the contribution will be smaller and smaller as the dissipated energy approaches zero. However, except for the difference in magnitude, the difference in the shape of the two relationships is relatively small.

The contribution to the SDI from each cycle (ΔSDI_i) for selected laboratory specimens at different expansion levels is shown in Figure 7.1. According to this, the contribution of the first cycle, ΔSDI_1, increases with increasing expansion levels up to 2.5‰, which is where the progress in the results (SDI and E/E_{ref}) starts to level off. The contribution of ΔSDI_2-ΔSDI_5, however, not only increases up to expansion level 2.4‰, but from 2.4 to 4.1‰ as well. Specimens FP38-3-Z2 and FP38-4-Z1 have the same SDI despite their very different expansion levels; 2.4‰ and 4.1‰. If we compare these specimens, the ΔSDI_1 is somewhat lower at expansion 4.1‰ than at 2.4‰, while all the other ΔSDIs (ΔSDI_2-ΔSDI_5) are higher. For specimen FP38-4-Z2, which has the same expansion as FP38-4-Z1 and a little higher SDI, 0.25 versus 0.23, the contribution to the SDI from all the cycles is higher than for both specimen FP38-3-Z2 and specimen FP38-4-Z1. This shows that the correlation between the SDI values and the partial contribution of each cycle is quite good, but that the relationship between SDI and expansion probably could be better if only some of the cycles were included in the SDI. This will, however, depend on the expansion level. The first cycle is probably the most important at lower expansion levels, but it could be more sensitive to other effects at higher levels.

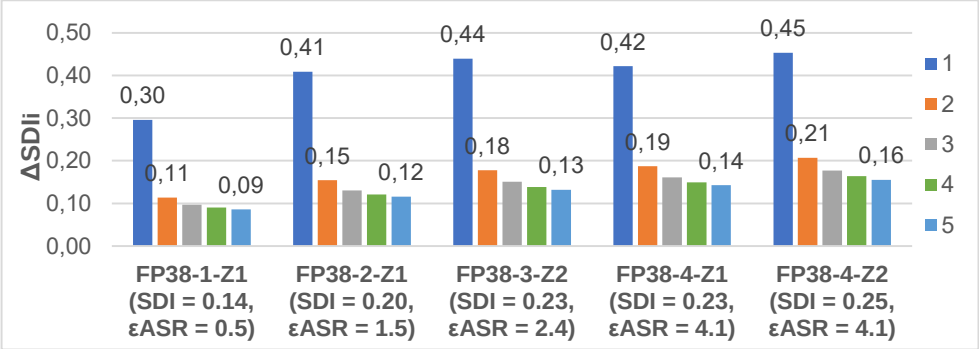

Figure 7.1: Ratio between dissipated and applied energy in each cycle (1-5) at different SDI and expansion levels in the laboratory specimens. The specimens are drilled from the free cubes stored at 38°C (FP38) at expansion levels 0.5 (FP38-1), 1.4 (FP38-2), 2.3 (FP38-3) and 4.1‰ (FP38-4).

The contribution of the different cycles to the SDI for selected specimens from Beam 1 and Plate 1 on Elgeseter Bridge is shown in Figure 7.2. The distribution for the four beam specimens (left in the figure) is about the same as for the laboratory specimens with corresponding SDI values. However, there is a tendency for the contributions from cycles two to five to be more similar in the field cores than in the laboratory specimens. Two of the specimens (b-A1-2-east and b-A1-2-west) are from the same core, but with slightly different SDIs. As the figure shows, the higher SDI in the western specimen is a result of higher ΔSDI_2-ΔSDI_5. The SDIs for the two plate specimens (right in the figure), 0.33 and 0.37, are much higher than any of the laboratory specimens in Figure 7.1. Typical for these plate specimens is that the contribution to SDI is higher in all cycles, but especially the first.

The correlation between SDI and E/E_{ref} can be shown if the average SDI values are plotted versus the corresponding E/E_{ref} values. This is done to the left in Figure 7.3 for both the laboratory and Elgeseter specimens. As the figure shows, the correlation between SDI and E/E_{ref} is largely congruent in the two test series, and the relationship is also quite linear. This last condition shows that both methods are suitable for the expansion estimate.

The expansion in the free direction for the various structural parts of Elgeseter Bridge in Locations A, B and C, was estimated based on both the SDI and the E/E_{ref} correlation with the expansion for the laboratory specimens, as shown in Figure 6.2. Overall, the two methods estimate quite similar expansions. However, the E/E_{ref} method results in lower estimates of expansion than the SDI method when the degree of deterioration (and estimated free expansion) is low ($E/E_{ref} > 0.9$, $\varepsilon ASR < 1.0‰$), as shown by Beam 2 in all locations. This deviation is probably a general problem since this correlation starts from $E/E_{ref} = 1.0$. If this relation is quite linear, the corresponding expansions at the beginning will be small. The SDI relation is therefore more applicable in this range since it starts from a certain point (0.08 for the laboratory specimens). The opposite situation, i.e., when the E/Eref correlation gives higher expansions than the SDI relation, appears for the structural parts Beam 1/Area C and Plate 2/Area A,

where the degree of deterioration and estimated expansion is higher (E/E_{ref} ~ 0.6, εASR = 1.5-3.2‰). However, this may be due to specific conditions related to individual specimens in these series of tests. For the test series Beam 1/Area C, one of the four specimens has a significantly lower SDI than the other specimens, even though the E-moduli are quite equal. For Plate 2/Area A, the results are based on one single specimen, for which the E-modulus of the fifth cycle is somewhat lower than expected compared to other specimens with similar SDI. These two series of tests (Beam 1/Area C and Plate 2/Area A) can be seen as the two points far to the left from the regression lines in Figure 7.1.

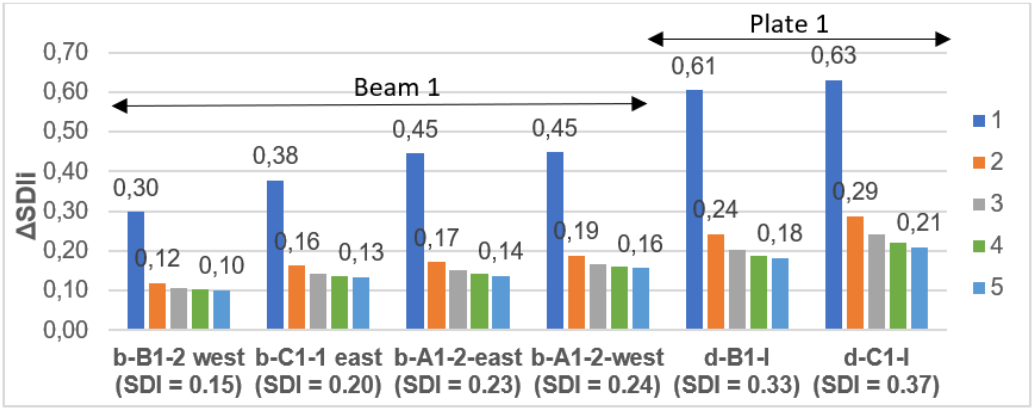

Figure 7.2: Ratio between dissipated and applied energy in each cycle (1-5) at different SDI levels of specimens from on Elgeseter Bridge. The selected specimens from Beam 1 are the western part from the second core in location B (b-B1-2 west), eastern part of the first core in location C (b-C1-1 east), and the eastern and western part of the second core from location A (b-A1-2 east, b-A1-2 west). The specimens from Plate 1 are from location B (d-B1-I) and C (d-C1-I), respectively.

The need for a reference E-modulus is also a challenge for the E/Eref ratio since this value is necessarily not so easy to determine in an existing structure. However, due to the good correlation between the SDI and the E/E_{ref} ratio in laboratory tests, a reasonable value can be determined from the linear relationship in Figure 7.3. Nevertheless, the estimation of expansions in Elgeseter Bridge in the rest of this paper are based on the average SDI-expansion correlation. Two alternative methods of calculating the SDI was also used: 1) by considering just the second cycle (ΔSDI_2), and 2) by summing the contribution from each cycle (ΔSDI_1-ΔSDI_5). The estimated expansion based on these results were in good agreement with the estimated expansions based upon the SDI from all the cycles, calculated in accordance with Equation (1). This is as expected since they are based on the same expansion values from the laboratory specimens. The two alternative methods are therefore not considered further in this paper, even though they also show interesting results.

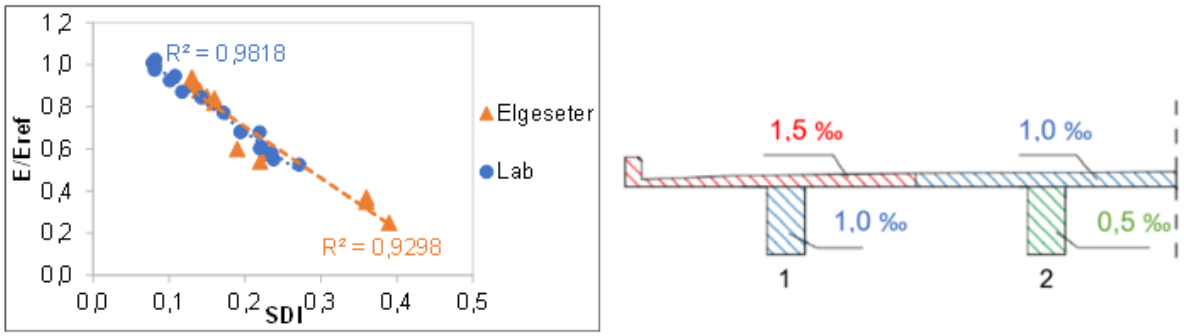

Figure 7.3: Left: Relation between E/E_{ref} and SDI of the laboratory and Elgeseter test. The blue labels represent the laboratory tests and the orange the Elgeseter tests. Right: Expansion distribution used for assessing additional load effects on Elgeseter Bridge

For Beam 1 and Beam 2, the sectional (A, B and C) estimated expansion values are 2.4, 0.7 and 1.5‰ and 0.6, 0.6 and 0.9‰, respectively. The corresponding estimated expansion values for Plate 2 are 2.1, 1.0 and 0.8‰, as shown in Figure 6.2. For Plate 1, the average SDI results of the cores from Location

A, B and C, are 0.36, 0.36, and 0.39, respectively. These values lie beyond the range of the laboratory curves, in which the highest SDI was about 0.27 for an expansion of about 3.7‰. The estimated expansions in Figure 6.2 from this member are based upon an extension of the linear relationship that was initially only applicable for expansion levels up to about 2.5‰. So, it is not possible to determine a reliable expansion for Plate 1. Plausible reasons for the high SDI for these specimens, as shown in Figure 7.2, may be that the stiffness properties of the alkali gel in the field specimens are different from the laboratory specimens or that there may be additional damage in the specimens. The damage observed at the surface of these cores was more extensive than in cores from Plate 2 and the beams, with clear signs of ASR gel and reaction rims around aggregates and, in some cases, relatively large cracks. This agrees with previous findings reported by Rodum et al. [11]. The SDT does not distinguish between ASR damage and damage from other deterioration mechanisms. Frost may lead to additional cracks in the concrete that are not necessarily filled with gel, but which can increase the internal friction in the material and result in higher energy dissipation in the SDT. Smaoui et al. [3] showed that specimens subjected to freeze-thaw gave higher energy dissipation from the SDT than specimens subjected to ASR at similar expansion levels. These issues should be further investigated, but effects other than ASR have probably contributed to the high SDI in Plate 1. Nevertheless, it should be mentioned that the results for the plate are based on a smaller number of specimens than the results for the beams, making them more uncertain.

Sanchez et al. [6] argued that the loading level (in % of compressive strength) and the l/d ratio were among the most important parameters with regard to the SDT results. However, neither the differences in l/d ratio nor the loading level seems to give a specific pattern in the field results in this case. One general trend is that the specimens with the highest SDI also had the highest load levels, but this is because the reference compressive strength was correspondingly reduced at the various locations. For Beam 1 in Areas A and C, where the compressive strength was lower than expected, one of the three specimens from the same core was tested at 12 MPa instead of 16 MPa. However, this only gave a slight reduction in the SDI value of the least loaded specimen. The scatter was also relatively low for the specimens from this core. Since the cores from Plate 1 had apparent signs of damage and lower compressive strength, the applied stress was also 12 MPa for all these specimens, as shown in Table 6.1. Measuring lengths shorter than 100 mm were only used for the specimens from Plate 1. The effect of this, however, seems to be small, as both the specimens from Area B and Area C of this plate had one core with 80- and 65-mm measuring length and they all got about the same results.

Elgeseter Bridge has recently been assessed for additional load effects caused by the ASR expansion [15]. The distribution of the expansion in the longitudinal direction of the bridge was then assumed to be as shown to the right in Figure 7.3. The calculated elongation based on this distribution corresponds well with the assumed global elongation of 200 mm for this bridge. Only half of the cross-section is shown in this figure since the expansion was assumed to be symmetrical about the middle line. The inner beam (Beam 2) and plate (Plate 2) were assumed to have an expansion of 0.5‰ and 1‰, respectively, while the outer parts of the cross-section (Beam 1 and Plate 1) were assumed to have 0.5‰ more in each part, i.e., 1.0‰ in Beam 1 and 1.5‰ in Plate 1. The transitions between each part are probably not this clear, and the local variations are also expected to be large.

The average estimated expansion of all the three locations in Figure 6.2 is 1.5, 0.7, and 1.3‰ for Beam 1, Beam 2 and Plate 2, respectively. These values, however, were based on tests in the free (transversal/vertical) direction of each part. Due to the restraining effect of the reinforcement and the compressive stresses in various parts of the section along the bridge, the real expansion is expected to be somewhat smaller in the longitudinal direction. The scatter observed between the different locations and the different parts of the cross section is also expected to be smaller. The ratios between the estimated and previously predicted expansion were 0.67, 0.71 and 0.77, results which are in accordance with the effect of the reinforcement and the compressive stress in a test series in progress. The estimated expansions from the laboratory tests therefore fit quite well with the assumed distribution of the expansion used in the previous calculations. It is possible that loading in one direction could affect the deformation during the SDT due to less cracking in the transversal direction [2, 8]. The curves from the lab specimens in Figure 6.1 consider the transversal direction of the loaded cubes (grey points) since they appear to have similar results as the free cubes at the same expansion levels. The effect of the reinforcement and additional loading will be discussed in another paper.

8. SUMMARY AND CONCLUSIONS

The main objective of this investigation was to establish a relationship between two different damage parameters and the expansion for a typical ASR-affected Norwegian concrete that can be used to estimate the expansion in corresponding existing structures. The parameter study was carried out on laboratory specimens that were especially adapted to a typical bridge concrete from the 1950-60s and that was stored moist at 38 °C during the expansion. The main damage parameters investigated were the SDI and the E/E_{ref} ratio, which were determined on ø95 mm x 190 mm cylinders drilled from 230 mm test cubes at selected expansion levels up to about 4.0‰.

The cores were drilled from various parts of Elgeseter Bridge at three different locations, denoted A, B and C. They were drilled in the free directions transversal to the beams and normal to the plate. Three specimens were made from each core from the beams and one specimen from each core from the plate. The dimensions of the beam specimens were, as for the laboratory specimens, ø95 mm x 190 mm, while the length varied between 120 and 190 mm for the plate specimens. The measuring length during testing was adjusted correspondingly. The variation in measuring lengths, however, did not seem to influence the SDI values.

Both the SDI and the E/E_{ref} showed quite linear progression with the expansion up to about 2.5‰, before levelling off. The correlation between the two methods was also quite good. The SDI is assumed to be best suited for estimation of expansions up to about 2.0‰, while the E/E_{ref} ratio may be better at higher expansion levels. However, the expansions on Elgeseter Bridge estimated based on the SDI relationship were found to be the most reliable. Some possible modifications of the SDI method are discussed in the paper, e.g., just including some of the cycles or accumulating the partial damages of each cycle, but the significance of these alternative SDI expressions was found to be small.

In this paper, we assumed the relationship between the SDI and the expansions of the laboratory specimens would also apply to the specimens from the bridge. The scatter is quite large between the different parts of the bridge. The sectional (Areas A, B, C) estimated expansion values in the outer and inner beams were 2.4, 0.7 and 1.5‰ and 0.6, 0.6 and 0.9‰, respectively. These values were estimated based on the average SDI of several test specimens. The corresponding sectional expansion values in the inner part of the plate were 2.1, 1.0 and 0.8‰. It was not possible to estimate the expansion in the outer part of the plate, since all the SDI values obtained were outside the SDI values of the laboratory specimens. This is the moistest part of the plate, and one possible reason for the high SDI values is that this concrete has suffered from freeze-thaw cycles in addition to ASR expansion.

The average expansion in the outer and inner beams and the inner part of the plate was estimated to 1.5, 0.7 and 1.3‰, respectively. This is in the free direction of each part and we assumed that the expansion in the longitudinal direction of the bridge would be significantly lower due to the effect of the reinforcement and the compressive stresses in that direction. These values were assumed to be 1.0, 0.5 and 1.0‰ in a previous assessment of Elgeseter Bridge, which corresponds well with the measured 200 mm global elongation of the superstructure. Although the behaviour at low values of SDI seems to be relatively equal for the bridge and the lab series, there may be a systematic difference in the corresponding expansion. One criterion must therefore be that the concrete in the reference test series needs to be quite equal to that in the real structure. So, it seems the SDT method can be used to determine a reasonable ASR expansion in existing structures. However, this method does not distinguish between expansion due to ASR or other deterioration mechanisms. Supplementary examinations to assess ASR damage are therefore desirable.

Acknowledgements

The project is based at the Norwegian University of Science and Technology (NTNU) in Trondheim and is funded by the Norwegian Public Roads Administration and NTNU. Both the financial support and the engaged discussions are gratefully acknowledged. We also owe a big thank-you to SINTEF, who contributed with the preparation and testing of the concrete specimens.

References:

1. Crouch RS, Wood JGM (1990) Damage evolution in AAR affected concretes. Engineering Fracture Mechanics 35(1-3):211-218. https://doi.org/10.1016/0013-7944(90)90199-Q

2. Chrisp TM, Waldron P, Wood JGM (1993) Development of a non-destructive test to quantify damage in deteriorated concrete. Magazine of Concrete Research 45(165):247-256. https://doi.org/10.1680/macr.1993.45.165.247

3. Smaoui N, Bérubé, M-A, Fournier B, Bissonnette B, Durand B (2004) Evaluation of the expansion attained to date by concrete affected by alkali–silica reaction. Part I: Experimental study. Canadian Journal of Civil Engineering 31(5):826-845. https://doi.org/10.1139/l04-051

4. Bérubé M-A, Smaoui N, Fournier B, Bissonnette B, (2011) Evaluation of the expansion attained to date by concrete affected by alkali–silica reaction. Part III: Application to existing structures. Canadian Journal of Civil Engineering 32(3):463-479. https://doi.org/10.1139/l04-104

5. Sanchez LFM, Fournier B, Jolin M, Bastien J (2014) Evaluation of the stiffness damage test (SDT) as a tool for assessing damage in concrete due to ASR: Test loading and output responses for concretes incorporating fine or coarse reactive aggregates. Cement and Concrete Research 56:213-229. https://doi.org/10.1016/j.cemconres.2013.11.003

6. Sanchez LFM, Fournier B, Jolin M, Bastien J (2016) Practical use of the Stiffness Damage Test (SDT) for assessing damage in concrete infrastructure affected by alkali-silica reaction. Construction and Building Materials 125:1178-1188. https://doi.org/10.1016/j.conbuildmat.2016.08.101

7. Sanchez LFM, Fournier B, Jolin M, Mitchell D, Bastien J (2017) Overall assessment of Alkali-Aggregate Reaction (AAR) in concretes presenting different strengths and incorporating a wide range of reactive aggregate types and natures. Cement and Concrete Research 93:17-31. https://doi.org/10.1016/j.cemconres.2016.12.001

8. Sørgaard Kongshaug S, Oseland O, Kanstad T, Hendriks MAN, Rodum E, Markeset G (2020) Experimental investigation of ASR-affected concrete –The influence of uniaxial loading on the evolution of mechanical properties, expansion and damage indices. Construction and Building Materials 245, 118384. https://doi.org/10.1016/j.conbuildmat.2020.118384

9. Giannini ER, Folliard KJ (2012) Stiffness damage and mechanical testing of core specimens for the evaluation of structures affected by ASR, in Proceedings of the 14th International Conference on Alkali–Aggregate Reaction in Concrete.

10. Jensen V (2003) Elgeseter Bridge in Trondheim Damaged by Alkali Silica Reaction: Microscopy, Expansion and Relative Humidity Measurements, Treatment with Mono Silanes and Repair, in 9th Euroseminar on Microscopy Applied to Building Materials.

11. Rodum E, Pedersen BM, Relling RH (2016) Field and laboratory examinations of an ASR-affected bridge – Variation in crack extent and water content, in the 15th ICAAR Conference.

12. Østmoen T (2013) Elgeseter Bridge. Report from special survey 2012 for Dr. Ing. A. Aas-Jakobsen AS (in Norwegian).

13. Lindgård J, Nixon PJ, Borchers I, Schouenborg B, Wigum BJ, Haugen M, Åkesson U (2010) The EU "PARTNER" Project – European standard tests to prevent alkali reactions in aggregates: Final results and recommendations. Cement and Concrete Research 40: 611-635. https://doi.org/10.1016/j.cemconres.2009.09.004

14. Oseland O (2018) The effect of accelerated ASR on the mechanical properties and degree of damage of concrete over time - with and without uniaxial compressive stress. Master thesis, NTNU. http://hdl.handle.net/11250/2572908

15. Nordhaug KO, Stemland KM (2018) Beregning av bru med alkalireaksjoner : Tilstandsvurdering og kapasitetskontroll av Elgeseter bru [in Norwegian]. Master thesis, NTNU. http://hdl.handle.net/11250/2568090